

THE KPNO INTERNATIONAL SPECTROSCOPIC SURVEY.  
II. H $\alpha$ -SELECTED SURVEY LIST 1.

JOHN J. SALZER<sup>1,2</sup> AND CARYL GRONWALL<sup>1,3</sup>

Astronomy Department, Wesleyan University, Middletown, CT 06459; slaz@astro.wesleyan.edu

VALENTIN A. LIPOVETSKY<sup>1,4</sup> AND ALEXEI KNIAZEV<sup>1</sup>

Special Astrophysical Observatory, Russian Academy of Sciences, Nizhny Arkhyz,  
Karachai-Circassia 357147, Russia; akn@sao.ru

J. WARD MOODY

Department of Physics & Astronomy, Brigham Young University, Provo, UT 84602;  
jmoody@astro.byu.edu

TODD A. BOROSON

National Optical Astronomy Obs., P.O. Box 26732, Tucson, AZ 85726; tyb@noao.edu

TRINH X. THUAN

Astronomy Department, University of Virginia, Charlottesville, VA 22903;  
txt@starburst.astro.virginia.edu

YURI I. IZOTOV

Main Astronomical Observatory, National Academy of Sciences of Ukraine, Goloseevo, Kiev 03680,  
Ukraine; izotov@mao.kiev.ua

JOSÉ L. HERRERO

BBN Technologies, Cambridge, MA 02140; jose@world.std.com

LISA M. FRATTARE<sup>1</sup>

Space Telescope Science Institute, Baltimore, MD 21218; frattare@stsci.edu

*To appear in The Astronomical Journal*

ABSTRACT

The KPNO International Spectroscopic Survey (KISS) is a new objective-prism survey for extragalactic emission-line objects. It combines many of the features of previous slitless spectroscopic surveys with the advantages of modern CCD detectors, and is the first purely digital objective-prism survey for emission-line galaxies. Here we present the first list of emission-line galaxy candidates selected from our red spectral data, which cover the spectral range 6400 to 7200 Å. In most cases, the detected emission line is H $\alpha$ . The current survey list covers a one-degree-wide strip located at  $\delta(1950) = 29^\circ 30'$  and spanning the RA range  $12^h 15^m$  to  $17^h 0^m$ . An area of 62.2 deg<sup>2</sup> is covered. A total of 1128 candidate emission-line objects have been selected for inclusion in the survey list (18.1 per deg<sup>2</sup>). We tabulate accurate coordinates and photometry for each source, as well as estimates of the redshift and emission-line flux and equivalent width based on measurements of the digital objective-prism spectra. The properties of the KISS emission-line galaxies are examined using the available observational data.

*Subject headings:* galaxies: emission lines — galaxies: Seyfert — galaxies: starburst — surveys

1. INTRODUCTION

The KPNO International Spectroscopic Survey (KISS) is an ongoing objective-prism survey which targets the detection of large numbers of extragalactic emission-line sources. The survey method is pat-

terned after previous surveys for these types of objects carried out with Schmidt telescopes and photographic plates (e.g., Markarian 1967, Smith *et al.* 1976, MacAlpine *et al.* 1977, Pesch & Sanduleak 1983, Wasilewski 1983, Markarian *et al.* 1983, Zamorano *et al.* 1994, Popescu *et al.* 1996, Surace & Comte

<sup>1</sup>Visiting Astronomer, Kitt Peak National Observatory. KPNO is operated by AURA, Inc. under contract to the National Science Foundation.

<sup>2</sup>NSF Presidential Faculty Fellow.

<sup>3</sup>present address: Department of Physics & Astronomy, Johns Hopkins University, Baltimore, MD 21218; caryl@adcam.pha.jhu.edu.

<sup>4</sup>Deceased 22 September 1996.

1998). The primary characteristic that distinguishes KISS from these previous surveys is that we utilize a CCD as our detector. With the advent of large format CCDs, the areal coverage possible with the combination of Schmidt telescopes and CCDs makes digital surveys like KISS both possible and highly desirable. The obvious advantages of CCDs over photographic plates include much higher quantum efficiency, lower noise, good spectral response over the entire optical portion of the spectrum, and large dynamic range. In addition, CCDs give us the ability to use automated selection methods to detect emission-line galaxies (ELGs), and allow us to quantify the selection function and completeness limit directly from the survey data. The combination of increased depth and large areal coverage is a powerful one, and allows for substantial improvements compared to the previous photographic surveys listed above.

The primary goal of KISS is to produce a high-quality survey whose selection function and completeness limits can be accurately quantified so that the resulting catalog of ELGs will be useful for a broad range of studies requiring statistically complete galaxy samples. We also want to reach substantially deeper than previous objective-prism surveys.

A complete description of the survey method employed for KISS is given in the first paper in this series (Salzer *et al.* 2000, hereafter Paper I). As described there, the first survey strip was observed in two distinct spectral regions. One covered the blue portion of the spectrum (4800 – 5500 Å), while the second covered the wavelength range 6400 – 7200 Å in the red part of the spectrum. The first blue survey list is given in Salzer *et al.* (2001, hereafter KB1). The present paper presents the initial KISS list of H $\alpha$ -selected ELG candidates. In addition to listing the ELGs, we provide substantial observational data for each object. This includes accurate photometry and astrometry for each source, as well as estimates of each galaxy’s redshift, line flux, and equivalent width. These data are used to examine the properties of the KISS ELGs in Section 4.

## 2. OBSERVATIONS

All survey data were acquired using the 0.61-meter Burrell Schmidt telescope<sup>5</sup>. The detector used for all data reported here was a 2048 × 2048 pixel STIS CCD (S2KA). This CCD has 21- $\mu$ m pixels, which yielded an image scale of 2.03 arcsec/pixel. The overall field-of-view was 69 × 69 arcmin, and each image covered 1.32 square degrees. The red survey spectral data were obtained with a 4° prism, which provided

a reciprocal dispersion of 24 Å/pixel at H $\alpha$ . The spectral data were obtained through a special filter designed for the survey, which covered the spectral range 6400 – 7200 Å (see Figure 1 of Paper I for the filter transmission curve).

The survey data consist of the spectral images, obtained with the objective-prism on the telescope, plus direct images taken without the prism through standard B and V filters. The first survey strip was initially observed only in the blue spectral region (KB1). The primary emission line detected in the blue survey data is [O III] $\lambda$ 5007. This first blue survey consists of a contiguous strip of fields observed at a constant declination ( $\delta(1950) = 29^\circ 30'$ ). The R.A. range covered is 8<sup>h</sup> 30<sup>m</sup> to 17<sup>h</sup> 0<sup>m</sup>. This area was chosen to overlap completely the Century Redshift Survey (Geller *et al.* 1997). After experiments with spectral observations in the red indicated great promise, we began re-observing the same fields, obtaining spectral images with the prism and filter combination listed above. The red survey used the existing direct images obtained for the blue survey strip. Limited observing time prevented us from reobserving the entire strip in the red; only 54 of the 102 fields of the initial blue strip were observed in the red. These fields fall in the R.A. range 12<sup>h</sup> 15<sup>m</sup> to 17<sup>h</sup> 0<sup>m</sup>, but exclude three fields near the middle of this strip from 14<sup>h</sup> 30<sup>m</sup> to 14<sup>h</sup> 45<sup>m</sup>.

The spectral data used for this paper were obtained during two observing runs. The first occurred in 1997 May 3–6, when objective-prism images of 20 survey fields were obtained, and the second in 1997 June 5–12, when an additional 34 fields were observed. The observations of the direct images will be described more completely in KB1; the same set of direct images was used for both KB1 and the current red spectral survey. The CCD used on the Burrell Schmidt was replaced after the 1997 June run, making additional red spectral observations of the existing survey fields less desirable. Subsequent observations with the new CCD have focused on new survey regions.

All red spectral data consist of four 720 s exposures of each field, for a total exposure time of 48 minutes per field. The telescope is dithered by  $\sim 10$  arcsec between exposures in order to move sources off of bad columns/pixels on the CCD. Data processing procedures are detailed in Paper I. The analysis of the survey data is carried out using an IRAF<sup>6</sup>-based software package written by members of the KISS team. This package is described in Herrero *et al.* (2000).

<sup>5</sup>Observations made with the Burrell Schmidt of the Warner and Swasey Observatory, Case Western Reserve University. During the period of time covered by the observations described here, the Burrell Schmidt was operated jointly by CWRU and KPNO.

<sup>6</sup>IRAF is distributed by the National Optical Astronomy Observatories, which are operated by AURA, Inc. under cooperative agreement with the National Science Foundation.

### 3. LIST 1 OF THE KPNO INTERNATIONAL SPECTROSCOPIC SURVEY

#### 3.1. Selection Criteria

The KISS reduction software selects ELG candidates by searching the extracted objective-prism spectra for objects possessing  $5\sigma$  emission features. That is, objects must possess one or more pixels with a flux level more than five times the total noise (Poissonian plus instrumental) above the neighboring continuum level in order to be selected for inclusion. This is the primary selection criterion of the survey. After the automated selection process is completed, the candidate ELGs are checked manually by examining both their extracted spectra and their appearance in the spectral and direct images. Many spurious sources are rejected at this stage. These often consist of objects in which spikes have been introduced during spectral overlap corrections (see *Herrero et al.* 2000), bright stars which possess spectral breaks within the KISS bandpass that can mimic an emission line (e.g., M stars), and very faint objects with residual cosmic rays present. Typically,  $\sim 80$  objects per field are identified as ELG candidates by our automated software, but roughly 70% are rejected as spurious during this checking process. When the nature of a potential ELG is not clear from examination of its spectrum, we also consider other information to help assess whether or not it should be retained in the sample. Useful parameters in this process include the B–V color and the object classification. For example, objects classified as stars that also have very red colors are usually rejected as being spurious sources. We stress that we do not require that an object be classified as a galaxy in order for it to be included in the final ELG list. Many of the objects included in the current list are unresolved in the direct images (which have an effective resolution of  $\sim 4$ – $5$  arcsec).

The visual examination of the spectral images also yields a number of objects that are missed by the automatic selection software but which do possess  $5\sigma$  emission features. These are typically objects with lines very close to the red end of the spectra, or bright galaxies with lower equivalent width lines where the continuum fitting process overestimates the continuum level slightly and hence underestimates the line strength. These objects are flagged manually as ELGs in the KISS tables. For the current survey list, 17.8% of the objects were added to the final catalog during this visual search. The combination of the automatic software and this visual checking ensures that the sample is quite complete for objects with  $\geq 5\sigma$  lines. A formal assessment of the survey completeness will be presented in *Gronwall et al.* (2000).

The  $5\sigma$  threshold level for inclusion in the survey

is a conservative value, one that was arrived at after substantial testing. While we wished to survey as deeply as possible, and include as many potential ELGs as possible, we also placed a high premium on the quality of the final survey lists. Early tests involving follow-up spectroscopy carried out on fields where objects were selected to lower thresholds showed that  $5\sigma$  detections were nearly always real sources, while objects between  $4\sigma$  and  $5\sigma$  tended to be real but also included a fair number ( $\sim 25\%$ ) of spurious sources. Below  $4\sigma$  the fraction of spurious sources increased dramatically. Hence, we selected  $5\sigma$  as the detection threshold for the survey. Objects with emission lines between  $4\sigma$  and  $5\sigma$  are also flagged in the database tables and retained as possible ELGs. However, this sample of  $<5\sigma$  sources is not statistically complete, and hence is not included in the main survey lists. Rather, we will include these additional lower probability sources in a secondary list of ELG candidates which should be thought of as a supplement to the main KISS catalog.

#### 3.2. The Survey

The list of ELG candidates selected in the first red survey is presented in Table 1. Because of the nature of the survey data, we are able to include a great deal of useful information about each source, such as accurate photometry and astrometry and estimates of the redshift and emission-line flux and equivalent width. Only the first page of the table is printed here; the complete table is available in the electronic version of the paper.

The contents of the survey table are as follows. Column 1 gives a running number for each object in the survey with the designation KISSR XXXX, where KISSR stands for “KISS red” survey. This is to distinguish it from the blue KISS survey (KB1). Future red survey lists will continue with this numbering scheme. Columns 2 and 3 give the object identification from the KISS database tables, where the first number indicates the survey field (FXXXX), and the second number is the ID number within the table for that galaxy. This identifier is necessary for locating the KISS ELGs within the survey database tables. Columns 4 and 5 list the right ascension and declination of each object (J2000). The formal uncertainties in the coordinates are 0.25 arcsec in RA and 0.20 arcsec in declination. Column 6 gives the B magnitude, while column 7 lists the B–V color. For brighter objects the magnitude estimates have uncertainties of typically 0.05 magnitude, increasing to  $\sim 0.10$  magnitude at  $B = 20$ . Paper I includes a complete discussion of the precision of both the astrometry and photometry of the KISS objects. An estimate of the redshift of each galaxy, based on its

objective-prism spectrum, in given in column 8. This estimate assumes that the emission line seen in the objective-prism spectrum is  $H\alpha$ . Follow-up spectra for >400 ELG candidates shows that this assumption is correct in the vast majority of cases. Only 8 ELGs with follow-up spectra are high redshift objects where a different line (typically [O III] and/or  $H\beta$ ) appears in the objective-prism spectrum. For objects with redshifts above  $z = 0.07$  the observed value is corrected as described in Paper I. The formal uncertainty in these redshift estimates is  $\sigma_z = 0.0028$ . Columns 9 and 10 list the emission-line flux (in units of  $10^{-16}$  erg/s/cm<sup>2</sup>) and equivalent width (in Å) measured from the objective-prism spectra. The calibration of the fluxes is discussed in Section 4.1.2. These quantities should be taken as being representative estimates only. A simple estimate of the reliability of each source, the quality flag (QFLAG), is given in column 11. This quantity, assigned during the line measurement step of the data processing, is given the value of 1 for high quality sources, 2 for lower quality but still reliable objects, and 3 for somewhat less reliable sources. Column 12 gives alternate identifications for KISS ELGs which have been cataloged previously. This is not an exhaustive cross-referencing, but focuses on previous objective-prism surveys which overlap part or all of the current survey area: Markarian (1967), Case (Pesch & Sanduleak 1983), Wasilewski (1983), and UCM (Zamorano *et al.* 1994). Also included are objects in common with the *Uppsala General Catalogue of Galaxies* (UGC, Nilson 1973).

A total of 1128 ELG candidates are included in this first list of KISS galaxies. The total area covered by the survey is 62.2 deg<sup>2</sup>, meaning that there are 18.1 KISS ELGs per deg<sup>2</sup>. This compares to the surface density of 0.1 galaxies per deg<sup>2</sup> from the Markarian survey, and 0.56 galaxies per deg<sup>2</sup> from the UCM survey; the present survey is much deeper! Of the total, 578 were assigned quality values of QFLAG = 1 (51.2%), 388 have QFLAG = 2 (34.4%), and 162 have QFLAG = 3 (14.4%). Based on our follow-up spectra to date, 100% (263 of 263) of the sources with QFLAG = 1 are *bona fide* emission-line galaxies, compared to 93% (111 of 119) with QFLAG = 2 and only 61% (28 of 46) with QFLAG = 3. The properties of the KISS galaxy sample are described in the next section.

Figure 1 shows an example of the finder charts for the KISS ELGs. These are generated from the direct images obtained as part of the survey. Figure 2 displays the extracted spectra derived from the objective-prism images for the first 24 ELGs in Table 1. Finder charts and spectral plots for all 1128 objects in the KISS survey are available in the electronic

version of this paper.

A supplementary table containing an additional 189 ELG candidates is included in the appendix of this paper (Table 2). These galaxies are considered to be lower probability candidates, having emission lines with strengths between  $4\sigma$  and  $5\sigma$ . Follow-up spectra of a limited number of these objects suggests that  $\sim 75\%$  are real ELGs, compared to  $\sim 94\%$  for the main KISS catalog. These additional galaxies do not constitute a statistically complete sample, and should therefore be used with caution. However, there are likely many interesting objects contained in this supplementary list, hence we include them for the sake of completeness.

#### 4. PROPERTIES OF THE KISS ELGS

A large amount of important observational information is available for each KISS ELG candidate from the survey data. This is due to the survey method employed for KISS, which includes the acquisition of photometrically-calibrated B and V direct images in addition to the objective-prism spectra. Furthermore, the digital nature of the spectral data allows us to more readily measure quantitative information from the spectra than was possible in previous photographic objective-prism surveys. Hence, a fairly complete picture of the survey constituents can be developed without the need for follow-up observations. Of course, the spectral information available from the objective-prism data is extremely coarse. One cannot, for example, distinguish between active galactic nuclei and star-forming galaxies based on the survey data alone. Follow-up spectra will be required in order to gain a more complete understanding of the nature of the KISS ELGs. Still, the available data can be used to investigate the properties of the survey constituents.

##### 4.1. Observed Properties

###### 4.1.1. Magnitude & Color Distributions

Figure 3a plots the histogram of B magnitudes for the 1128 KISS ELGs in the current survey list. The median apparent magnitude is 18.08. This compares to median apparent magnitudes of  $B = 16.9$  for the [O III]-selected Michigan (UM) survey (Salzer *et al.* 1989) and  $B \approx 16.1$  for the  $H\alpha$ -selected UCM survey (Pérez-González *et al.* 2000). Also indicated in the figure is the completeness limit of the Markarian survey,  $B = 15.2$  (Mazzarella & Balzano 1989). Clearly, the survey goal of creating a deep sample of ELGs has been achieved.

The distribution of B–V colors exhibited by the KISS sample is shown in Figure 3b. The median color of 0.67 is indicated. This median value, which is the typical color of an Sb galaxy (Roberts & Haynes

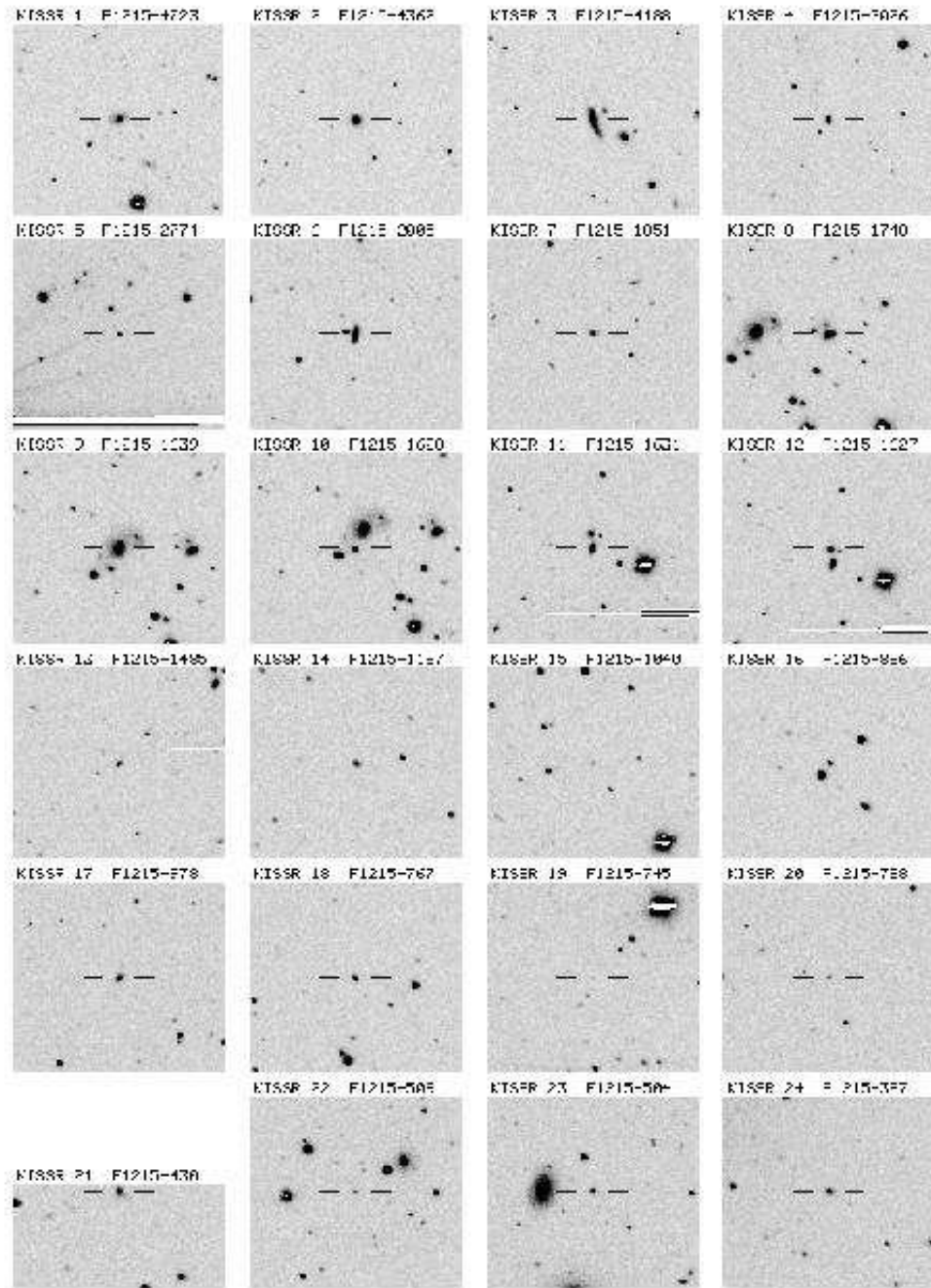


FIG. 1.— Example of finder charts for the KISS ELG candidates. Each image is  $4.5 \times 4.0$  arcmin, with N up, E left. These finders are generated from the direct images obtained as part of the survey. In all cases the ELG candidate is located in the center of the image section displayed, and is indicated by the tick marks.

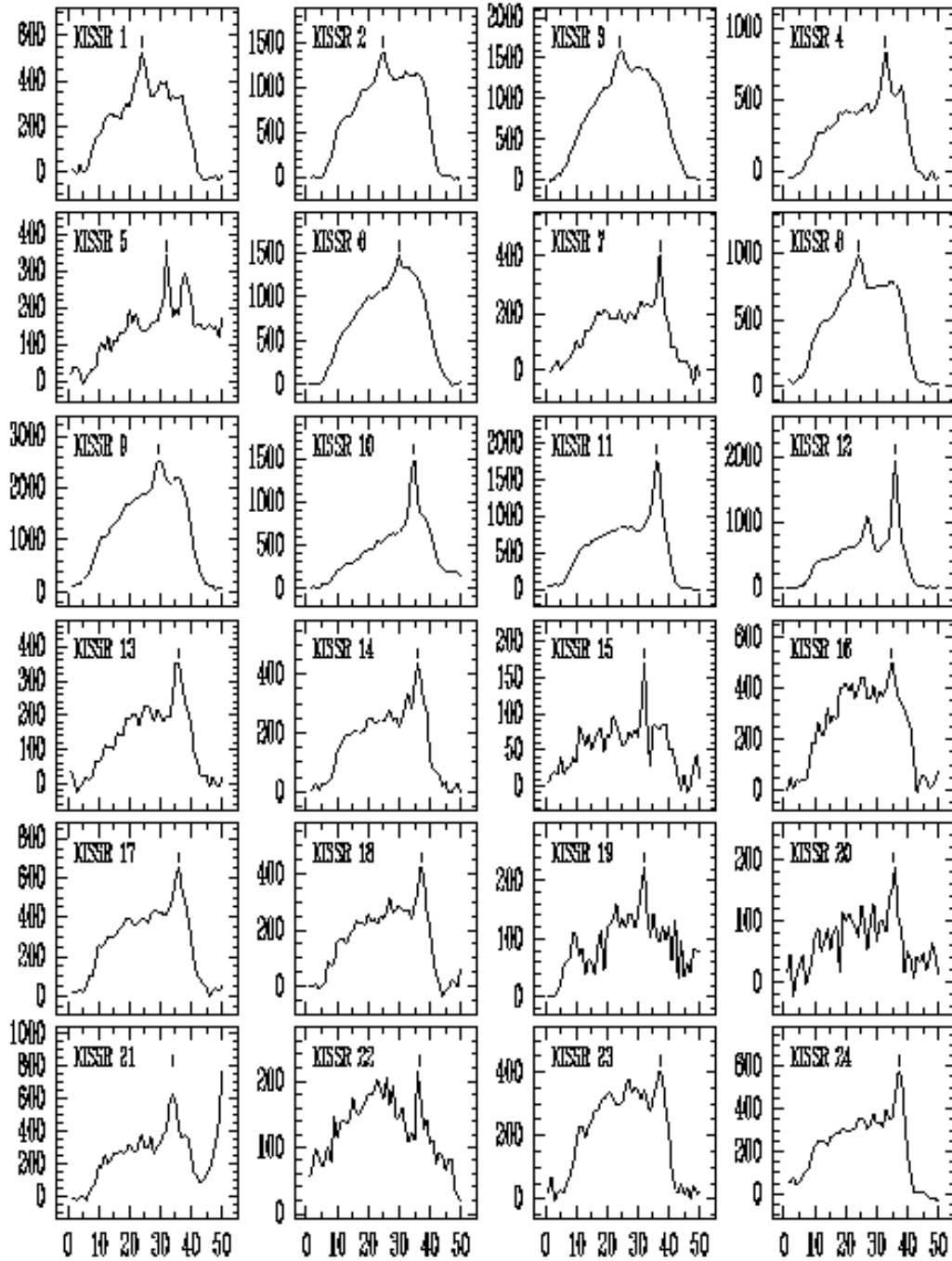


FIG. 2.— Plots of the objective-prism spectra for 24 KISS ELG candidates. The spectral information displayed represents the extracted spectra present in the KISS database tables. The location of the putative emission line is indicated.

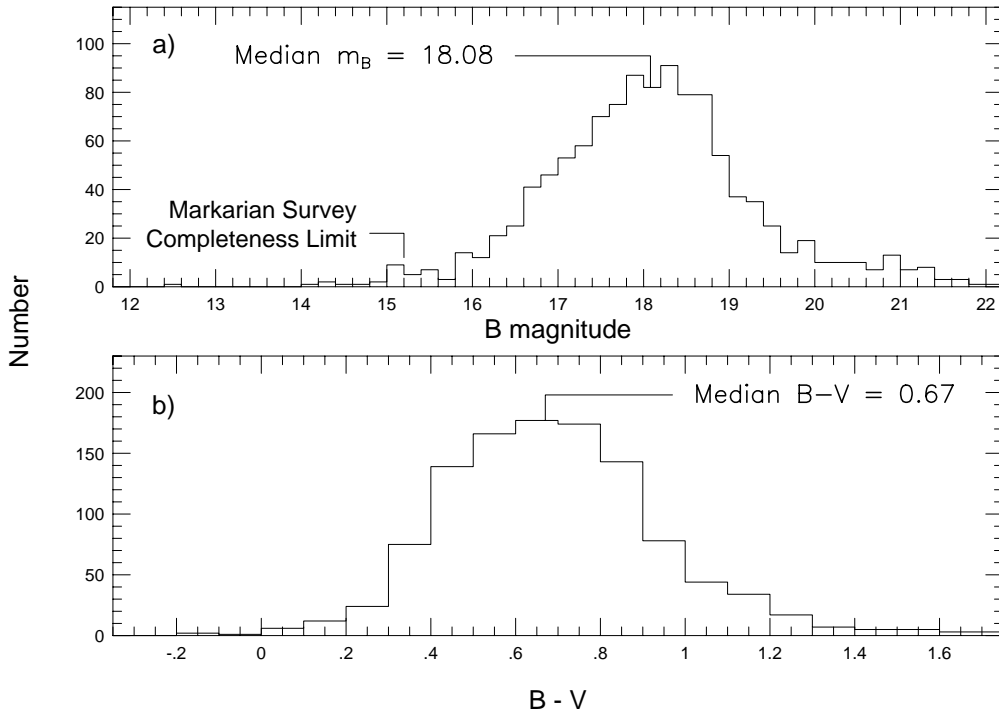


FIG. 3.— (a) Distribution of B-band apparent magnitudes for the 1128 ELG candidates in the first  $H\alpha$ -selected KISS survey list. The median brightness in the KISS sample is  $B = 18.08$ , with 7% of the galaxies having  $B > 20$ . Also plotted, for comparison, is the completeness limit of the Markarian survey. (b) Histogram of the  $B-V$  colors for the 1128 ELG candidates. The median color of 0.67 is indicated.

1994), is significantly redder than the median of  $B-V = 0.54$  for the UM survey (Salzer *et al.* 1989). This is most likely due to the differing selection criteria for the two surveys. The  $[O III]$ -selected UM survey preferentially detected lower luminosity ELGs with low amounts of reddening. While the  $H\alpha$ -selected KISS sample contains a large number of dwarf galaxies as well (see Section 4.2.1), it has a larger proportion of more luminous starburst galaxies and AGN. There is also a significantly weaker bias against heavily reddened ELGs with KISS compared to the UM or other blue-selected surveys. Hence the color range exhibited by the KISS sample is closer to that of the overall galaxian population. The color distribution appears to be similar to that of the UCM galaxies (Pérez-González *et al.* 2000), which have a mean  $B-r$  color of 0.71. This mean value is comparable to the mean color of an Sbc galaxy (Fukugita *et al.* 1995).

It is difficult at this time to assess the significance of the extended tail of very red ELGs. A total of 50 KISS galaxies in the current list possess  $B-V$  colors  $> 1.2$  (i.e., redder than any normal galaxy). Most of these objects are very faint: the median apparent

magnitude of these red objects is  $B = 20.6$ . At these magnitudes the uncertainties in the photometry are substantial (typical errors in the  $B-V$  color are 0.2 to 0.3 magnitude). Furthermore, the proportion of spurious sources increases at these faint magnitudes. Follow-up spectra will be required to confirm the nature of these very red objects. During our early spectroscopic follow-up observations, 14 of these red ELG candidates were observed, and only five have been confirmed as ELGs. The remainder are stars or faint galaxies with no emission lines. Hence, many of these red candidates are probably false detections. Of the five true ELGs mentioned above, three are Seyfert galaxies, which suggests that this red population of KISS objects harbors some interesting objects.

#### 4.1.2. Line Strength Distributions

As described in Paper I and Herrero *et al.* (2000), we are able to measure the position and strength of the emission line that is seen in the objective-prism spectrum of each KISS ELG. The line strength measurements, both line flux and equivalent width, yield useful quantitative information. This allows us to use

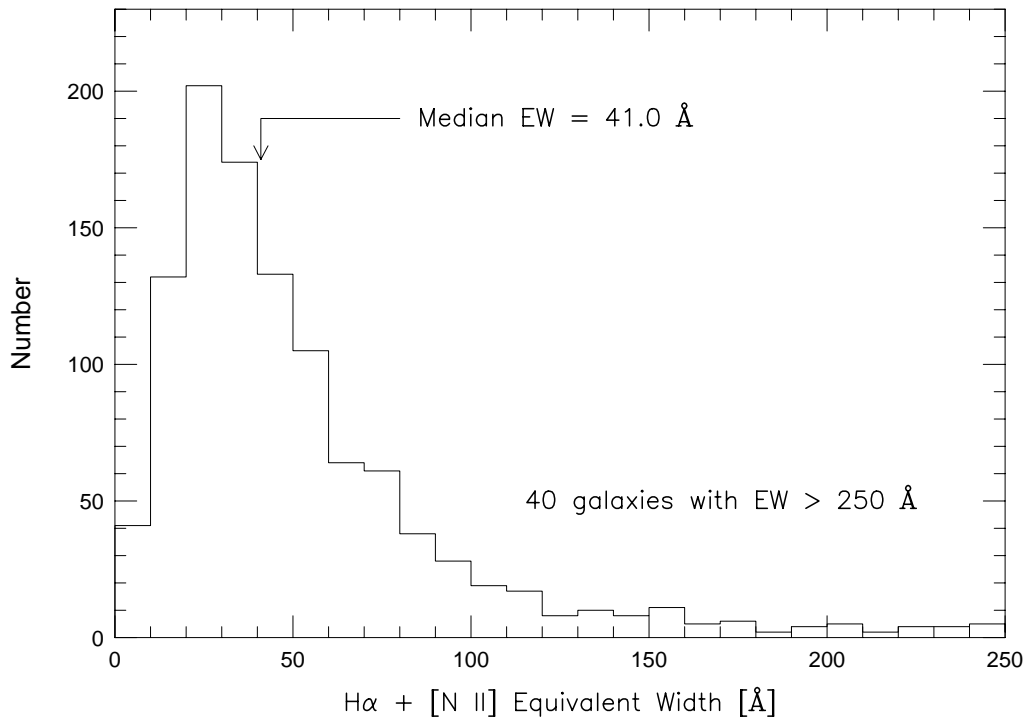


FIG. 4.— Distribution of measured  $H\alpha + [N II]$  equivalent widths for the KISS ELGs. The median value of 41 Å is indicated. The measurement of equivalent widths from objective-prism spectra tends to yield underestimates of the true equivalent widths, so these values should only be taken as estimates. The survey appears to detect most sources with  $EW(H\alpha + [N II]) > 30$  Å.

the survey data to assess the completeness of the survey. Since KISS is a line-selected survey, its completeness limit must be defined in terms of line strengths, not continuum apparent magnitudes (Salzer 1989). We discuss this issue further in Gronwall *et al.* (2000).

Given the low-dispersion nature of our spectra plus the low spatial resolution of the images, the measured line strengths are not as precise as those obtained from slit spectra. In particular, the nature of the objective-prism spectra makes the equivalent width estimate highly uncertain, due to the variable amount of underlying continuum flux present at the location of the line. Since light from all portions of the object gets dispersed by the prism, the location occupied by the emission line in the spectrum can have continuum contributions from a large area of the galaxy. Hence, for extended sources, the equivalent width measured from the survey spectra will tend to be significantly underestimated. This is not an important issue for compact objects. Partially compensating for this effect is the fact that our extracted spectra, which sum the flux over four pixels ( $\sim 8''$ ), tend to include all of the line emission from each source. This is in contrast to slit spectroscopy, where the 1–2'' slits typically em-

ployed can miss a large fraction of the line emission. Thus, the KISS line fluxes should yield fairly accurate estimates of the total  $H\alpha + [N II]$  emission.

The distribution of equivalent widths seen in our survey galaxies is plotted in Figure 4. We assume that the line we are measuring is  $H\alpha + [N II]$ . Based on our follow-up spectra to date (see Section 3.2), this appears to be a reasonable assumption. Due to our low spectral resolution, the  $[N II]\lambda\lambda 6584, 6548$  lines are always seen blended with  $H\alpha$ ; there is no way to determine the contribution from the individual lines using our survey data. We note in passing that the  $[S II]\lambda\lambda 6731, 6717$  doublet is well resolved from the  $H\alpha + [N II]$  complex, and is often seen in the objective prism spectra of strong-lined objects. The median equivalent width found from the current sample of ELGs is 41.0 Å. As can be seen in Figure 4, the vast majority of the galaxies have equivalent widths less than 100 Å. The distribution of EWs peaks in the 20–30 Å bin, suggesting that KISS is fairly complete for objects with EWs above  $\sim 30$  Å.

Calibrating the fluxes measured from the objective-prism spectra is crucial for scientific analyses such as determining the star formation rate of the local



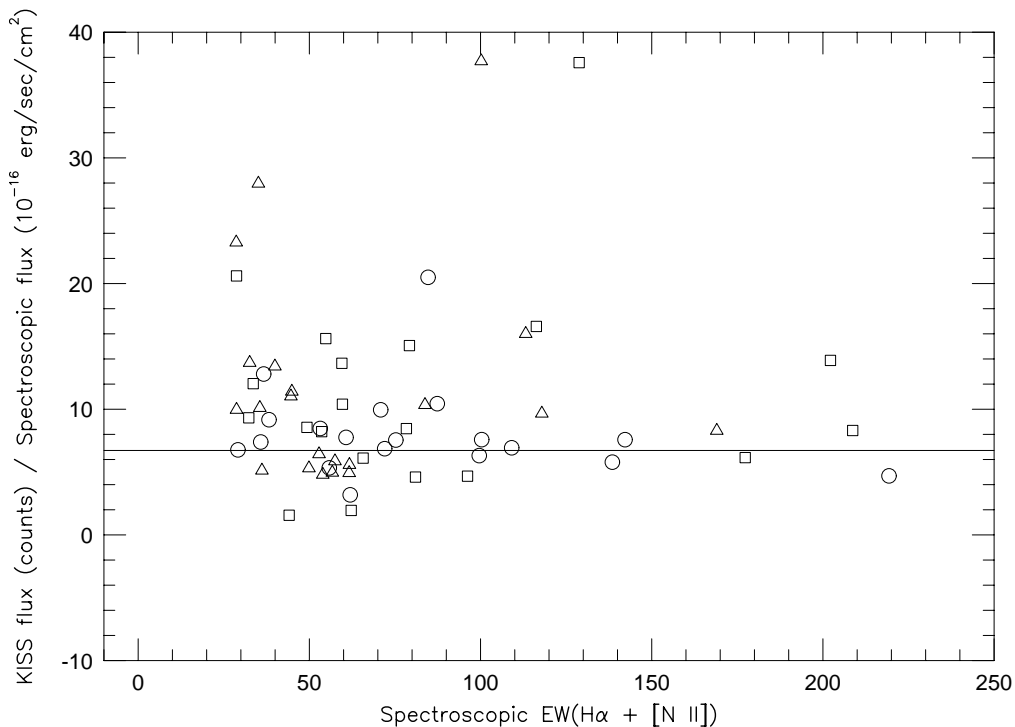


FIG. 5.— Plot of the ratio of objective-prism flux (in counts) to spectroscopic flux *versus*  $H\alpha + [N II]$  equivalent width measured from the follow-up spectra. Data from three different observing runs on two different telescopes are plotted: square = MDM 2.4-m in May, 1998, triangle = MDM 2.4-m in April, 1999, and circle = KPNO 2.1-m, May 1999. See Gronwall *et al.* (2001) for details of the spectroscopic observing runs. The solid line indicates the median ratio. Five galaxies with  $EW > 250 \text{ \AA}$  lie off the diagram to the right.

universe (Gronwall *et al.* 2000), as well as for establishing the completeness limit of the survey. The KISS line fluxes are calibrated in a two-step method. First, the objective-prism spectra for each field are corrected for throughput variations and atmospheric extinction (see Herrero *et al.* 2000). This places all line fluxes on the same *relative* flux scale. Then, the fluxes are calibrated using information obtained from our early follow-up spectra. Since the measured objective-prism line fluxes are often of low precision, due to the coarse nature of the spectra, the goal of the following calibration procedure was not necessarily to achieve high precision. Rather, an uncertainty of between 10 to 20% was considered acceptable.

We have obtained high-resolution follow-up spectra for 428 KISS candidates from the sample of 1128 presented in this paper. The spectroscopic observations will be described in Gronwall *et al.* (2001). For the purposes of calibrating the objective-prism spectra, we selected galaxies that are starbursting (i.e., not AGN), that had been observed with a longslit spectrograph under photometric conditions, and for

which high quality spectra were obtained. Galaxies observed through optical fibers were not used, since such spectra are notoriously difficult to use for accurate spectrophotometry. This limited our calibration sample to 65 galaxies. All data used were obtained using slit widths of either 1.7 or 2.0 arcsec. This guarantees that we recorded most of the emission-line flux from the sources, as long as the emission regions were not spatially extended. Since the fluxes measured from the objective-prism spectra are a combination of the  $H\alpha$  and  $[N II]$  lines, we used the fluxes from our slit spectra for the sum of these three lines. Figure 5 shows a plot of the ratio of objective-prism flux (in counts) to spectroscopic flux *versus* the equivalent width measured from the follow-up spectra. Data from three different observing runs on two different telescopes are plotted, and there are no obvious systematic trends in this ratio with either equivalent width or observing run. There are, however, a number of galaxies with large ratios, particularly at low equivalent width. A visual inspection of the survey images showed that these galaxies are of large angu-

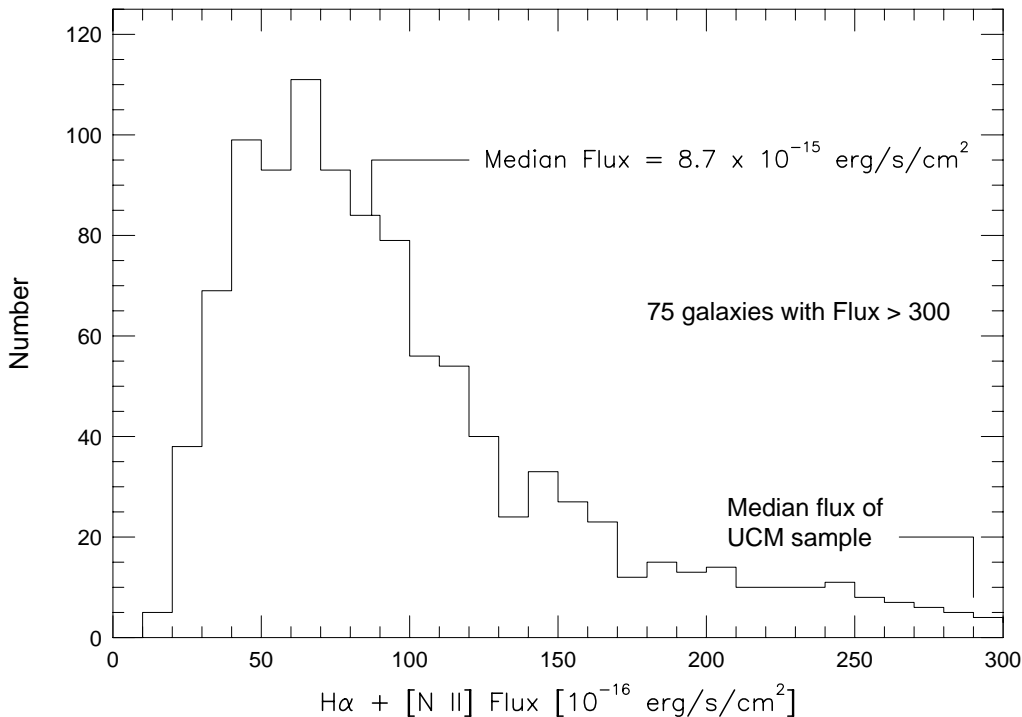


FIG. 6.— Distribution of  $H\alpha + [N II]$  line fluxes for the 1128 KISS ELGs included in the current survey list. The median flux level of both the KISS and UCM samples is indicated.

lar extent and exhibit extended line emission. The high flux ratios for these objects indicate that our longslit measurements do not include all of the  $H\alpha$  emission from these sources. Thus, we restricted our analysis to those galaxies with an objective-prism-to-spectroscopic flux ratio of less than 12.5 and an equivalent width greater than  $40 \text{ \AA}$ , leaving us with a calibration sample of 42 galaxies. These galaxies all possess emission regions that are essentially point sources. The median ratio of this sample was 6.72; the mean was 6.91 with a standard deviation of 2.48 and an error in the mean of 0.38. We have adopted as our calibration value the reciprocal of the median value, or  $0.1488 \times 10^{-16} \text{ ergs/sec/cm}^{-2}$  per count.

To check our calibration, we performed a similar analysis using the 17 galaxies from the UCM survey with spectral data in Gallego *et al.* (1996) that fall within our survey region. The KISS and UCM line fluxes are plotted in Figure 8 of Paper I. The resulting flux-ratio analysis for the UCM galaxies yields a median ratio of 6.62 and a mean ratio of 7.05, with a standard deviation of 1.09 and an error in the mean of 0.30. Thus the value agrees quite well (within 1.5%) with our derived calibration factor. Given the necessarily coarse nature of the objective-prism line

fluxes, we feel that the accuracy of our flux calibration method (formal error of 6%) is quite acceptable.

Figure 6 displays the histogram of observed  $H\alpha + [N II]$  line flux values for the 1128 KISS ELGs. The median value of  $8.7 \times 10^{-15} \text{ erg/s/cm}^2$  compares to that from the UCM sample of  $2.9 \times 10^{-14} \text{ erg/s/cm}^2$  (based on follow-up spectra of Gallego *et al.* 1996). A galaxy with this latter flux level would fall at the extreme right edge of the figure, which illustrates the increased depth of KISS relative to the UCM survey in terms of line flux.

#### 4.1.3. Redshift Distributions

The other parameter that we measure from the objective-prism spectra is the redshift of each object. The precision of the KISS redshifts is detailed in Paper I, where we show that the formal uncertainty in the KISS redshifts is  $0.0028$  ( $830 \text{ km s}^{-1}$ ). The distribution of the measured redshifts is illustrated in Figure 7. The upper panel shows the KISS ELGs, while the lower panel shows the distribution for 486 galaxies from Zwicky *et al.* (1961–1968; hereafter CGCG). The redshifts for the CGCG galaxies are taken from Falco *et al.* (1999); this is essentially the portion of the CfA2 redshift survey that covers the same area

on the sky as the KISS ELGs. Because the surface density of the CGCG catalog is fairly low, we have actually included objects lying in a four-degree-wide declination strip, rather than the one degree covered by KISS. The Falco *et al.* redshift catalog sample is complete to  $m_B = 15.5$ . This same comparison sample is used in the following section as well.

Compared to the CGCG sample, the KISS ELGs are detected in large numbers to much higher redshifts. The median redshift for the ELGs is more than double that of the magnitude-limited CGCG galaxies. There is a large void present between  $z = 0.038$  and  $0.054$  (see also Figure 9). Beyond this void, the number of KISS ELGs increases, while the CGCG galaxies remain sparse. Only a handful of luminous galaxies are present in the CGCG sample beyond  $z = 0.04$ . In contrast, the KISS ELGs increase in number out to the redshift limit imposed by the survey filter. The implications of this are (1) that the survey technique employed by KISS would be sensitive to galaxies at distances well beyond the distance limit imposed by the filter, if the filter was either not used or was replaced with one that extended to redder wavelengths, and (2) for the high-luminosity portion of the ELG luminosity function, the KISS sample is effectively volume-limited rather than flux-limited.

## 4.2. Derived Properties

### 4.2.1. Luminosity Distribution

We compare the luminosities of the KISS ELGs with those of the CGCG galaxies located in the same area of the sky in Figure 8. Absolute magnitudes are computed using the redshifts and apparent magnitudes listed in Table 1 and assuming a value for the Hubble Constant of  $H_0 = 75$  km/s/Mpc. Corrections for Galactic absorption ( $A_B$ ) have been applied by averaging the values for all UGC galaxies in each survey field from the compilation of Burstein & Heiles (1984). Since the majority of the survey strip is at high Galactic latitude, this correction is typically small: 31 of the 54 fields (57%) have  $A_B < 0.05$ , and 48 of 54 (89%) have  $A_B < 0.10$ . The maximum correction of  $A_B = 0.22$  occurs in the easternmost survey field (F1655). The median blue absolute magnitude of the KISS ELGs is  $-18.96$ , which is roughly one magnitude fainter than  $M^*$ , the “characteristic luminosity” parameter of the Schechter (1976) luminosity function. As seen in the lower portion of the figure, the majority of the CGCG galaxies are more luminous than the KISS ELGs. The median absolute magnitude of the CGCG sample is  $-20.08$  (i.e., very close to  $M^*$ ). Only 9.6% of the CGCG galaxies have luminosities below the median KISS luminosity.

Figure 8 reveals much about the KISS sample. It is dominated by intermediate- and low-luminosity

galaxies. The typical luminosity is comparable to the Large Magellanic Cloud. There is also a significant population of higher luminosity galaxies, but the high-luminosity end of the distribution is truncated relative to the CGCG sample. This is due to the volume-limited nature of the luminous end of the sample. Due to the filter-induced cut-off in the redshift distribution, the KISS sample lacks the high luminosity tail that is commonly seen in magnitude-limited samples.

Even though there are large numbers of lower luminosity ELGs present in KISS, the proportion of dwarf star-forming systems is significantly lower than in [O III]-selected surveys like the UM survey. The median absolute magnitude for the UM ELGs is  $M_B = -18.1$  (Salzer *et al.* 1989). Due to two factors – the way that the [O III] line strength varies with metallicity, and the luminosity-metallicity relation – [O III]-selected surveys have a selection function that peaks near  $M_B = -17$ . More luminous galaxies with starbursts tend to have weaker [O III] lines. In addition, [O III]-selected surveys tend to be biased against luminous galaxies due to the higher amounts of reddening present in these more metal-rich systems. Since KISS selects by  $H\alpha$ , it does not suffer from these biases. Hence, the KISS sample should be a more representative catalog of AGN and star-forming galaxies.

Despite the difference in the median luminosities of the UM and KISS samples, one should not conclude that the KISS sample is deficient in dwarf galaxies relative to the UM survey. Rather, the UM survey is missing a large fraction of the more luminous star-forming galaxies, which KISS recovers. This can be understood by consideration of the ELGs discovered in the first blue survey list (KB1). The luminosity distribution of the KB1 sample is nearly identical to that of the UM ELGs of Salzer *et al.* (1989). However, as discussed in Paper I, there is a tremendous overlap between the KB1 and current samples. In the regions where they overlap, 92% of the KB1 ELGs are also cataloged in the current paper (87% in the main catalog, and 5% in the supplementary list). Hence, the  $H\alpha$  survey technique is just as efficient at finding dwarf ELGs as is the [O III]-selection method. In addition, the  $H\alpha$ -selected samples detect many more higher-luminosity galaxies.

### 4.2.2. Spatial Distribution

Because of the depth and good redshift coverage of the KISS ELGs, it is also relevant to consider the spatial distribution of the sample. This is illustrated in Figure 9, which shows two cone diagrams for the KISS and CGCG galaxies. The redshifts plotted for the KISS galaxies are those from Table 1. Figure 9a shows all galaxies from both samples out to 15,000

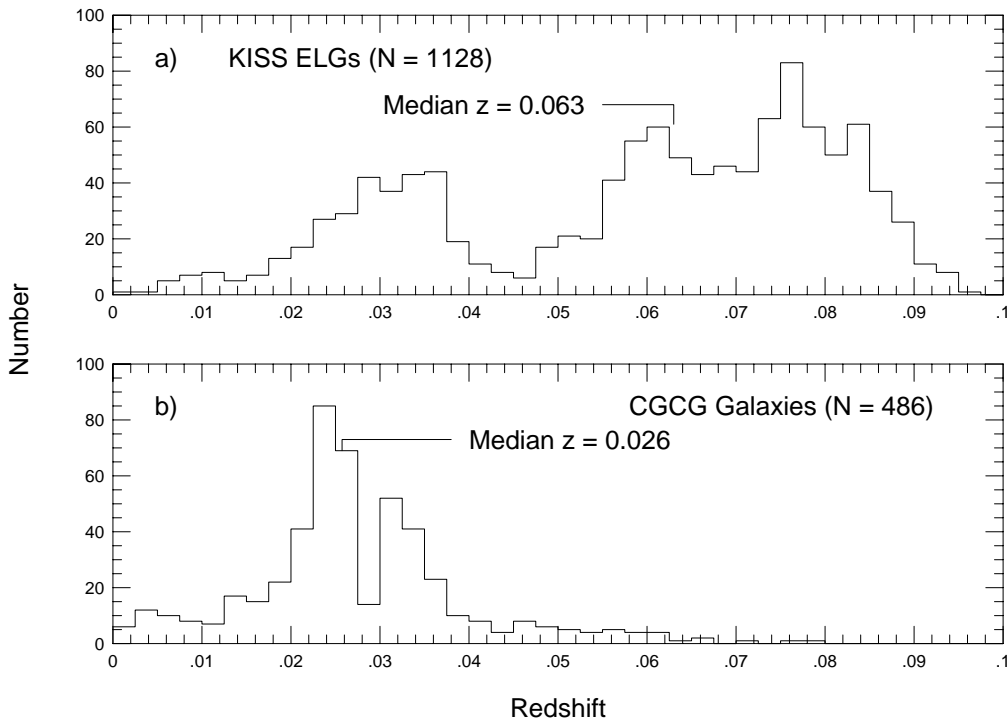


FIG. 7.— Histograms showing the distribution of redshift for (a) the 1128 H $\alpha$ -selected KISS ELGs and (b) the 486 “normal” galaxies from the CGCG which are located in the same area of the sky. The median redshift is indicated in both plots. Note that the number of KISS ELGs continues to rise up to the cut-off of the filter used for the survey, indicating that the survey is volume-limited for the more luminous galaxies. The deficit of ELGs between  $z = 0.038$  and  $0.054$  is due to a large void.

$\text{km s}^{-1}$  ( $z \leq 0.05$ ). The general impression obtained from examination of the figure is that the KISS ELGs tend to fall along the same large-scale structures seen at lower redshifts in the CGCG galaxies. However, the ELGs appear to be less tightly confined to the structures than are the “normal” galaxies. Because of the limited precision of the KISS redshifts ( $\pm 830 \text{ km s}^{-1}$ ; see Paper I), it is possible that the appearance of lower clustering is an artifact of the data. However, the large numbers of galaxies located well into some of the voids present within this volume of space suggest that the lower level of clustering is in fact real. Previous studies of the spatial distribution of ELG samples have found similar results (Salzer 1989, Rosenberg *et al.* 1994, Pustil’nik *et al.* 1995, Popescu *et al.* 1997, Lee *et al.* 2000). The lower level of clustering seen in Figure 9a is due primarily to lower-luminosity ELGs. We are currently analyzing the relative clustering strengths of the ELGs and CGCG galaxies, using more accurate redshifts from our follow-up spectra when available (Lee, Salzer & Gronwall 2001).

Figure 9b shows the galaxian distribution out to

$z = 0.10$ . At redshifts beyond about  $12,000 \text{ km s}^{-1}$ , the CGCG sample thins out drastically, and can no longer be used to delineate large-scale structure. The KISS galaxies, however, are found in great numbers out to  $\sim 27,000 \text{ km s}^{-1}$ , beyond which the survey is truncated abruptly by the filter. The ELGs in the cone diagram appear to indicate the presence of a number of filaments and voids at these higher redshifts. In fact, a comparison of Figure 9b with the similar diagram for the Century Redshift Survey (Geller *et al.* 1997) reveals that these apparent structures are real. The ELGs map out large-scale structures, albeit only roughly, out to  $z = 0.09$  without the need for follow-up spectra! While the limited velocity resolution, together with the tendency for the ELGs to be less clustered, prevents the use of these data for detailed definition of large-scale structures at these redshifts, they certainly provide a reasonable picture of the gross details. Furthermore, since the KISS galaxies are selected due to their strong line emission, follow-up spectroscopy of these faint galaxies is relatively easy. Thus, using ELGs to trace out the main features in the spatial distribution of galax-

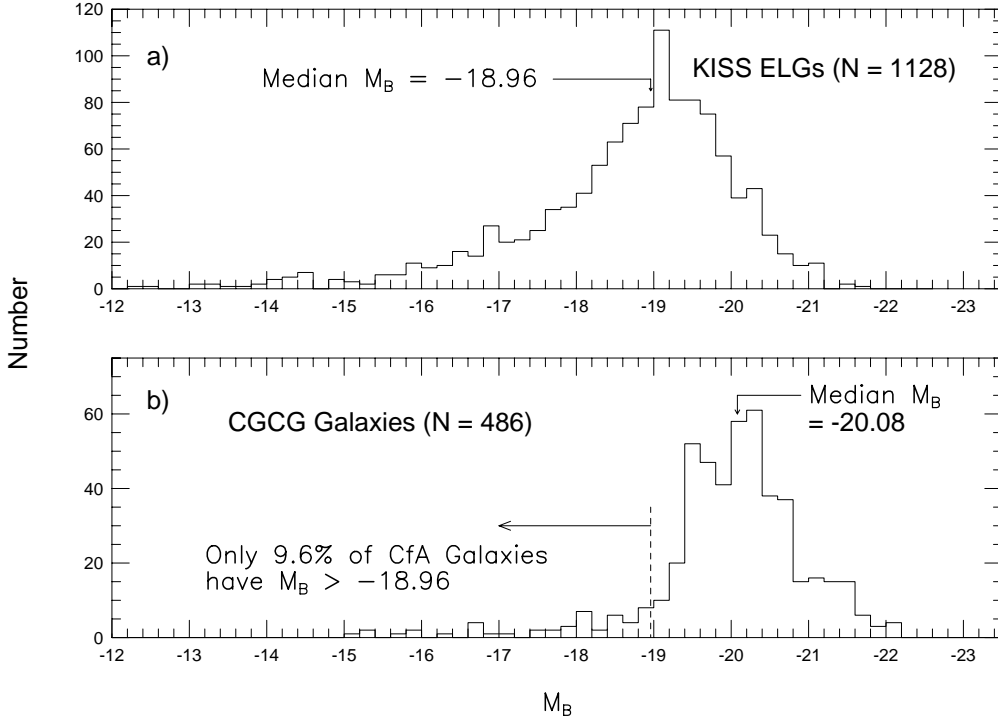


FIG. 8.— Histograms showing the distribution of blue absolute magnitude for (a) the 1128  $H\alpha$ -selected KISS ELGs and (b) the 486 “normal” galaxies from the CGCG that are located in the same area of the sky. The median luminosity of each sample is indicated. The KISS ELG sample is made up of predominantly intermediate- and lower-luminosity galaxies, making this line-selected sample particularly powerful for studying dwarf galaxies.

ies is an efficient use of telescope time.

#### 4.3. Comparison with Previous Surveys

Table 1 lists cross-references for KISS ELGs which are also cataloged in other surveys for active and star-forming galaxies. Four major surveys overlap the first red KISS strip: Markarian (1967), Case (Pesch & Sanduleak 1983), Wasilewski (1983), and UCM (Zamorano *et al.* 1994). It is instructive to consider the degree of overlap between these previous photographic surveys and KISS.

Two of the four surveys mentioned above are strictly line selected. The Wasilewski survey is [O III] selected, while UCM is  $H\alpha$  selected. The Markarian survey is UV-excess selected, while the Case survey is a hybrid of the two types: both line and UV-excess selected. One might then expect that KISS has the highest degree of overlap with the Wasilewski and UCM surveys. This is in fact the case. There are 8 Wasilewski galaxies within the area surveyed by KISS, and all 8 are recovered by KISS. Twenty five UCM galaxies reside in the KISS area, but follow-up spectroscopy by Gallego found that seven of these do

not possess emission lines. Hence, there are only 18 UCM galaxies with emission in the KISS area, and all 18 are found by KISS. Oddly enough, one of the seven UCM non-ELGs was recovered by KISS (KISSR 185 = UCM 1300+2959); a follow-up spectrum for this object has not yet been obtained.

While our first  $H\alpha$ -selected KISS list includes 100% of the ELGs from the previous line-selected surveys, it did not do as well with the UV-excess-selected surveys. There are seven Markarian galaxies in the survey area. Only four of these were recovered by KISS in the main survey (i.e., Table 1), while two additional objects are included in the supplementary list of  $4\sigma$  to  $5\sigma$  objects. The one Markarian survey galaxy not detected at all by KISS is Mrk 655 ( $B = 15.5$ ). Examination of its objective-prism spectrum shows no hint of an emission line. The redshift of Mrk 655 is less than the limit set by our survey filter, meaning that we did not miss it because the  $H\alpha$  line is redshifted beyond our spectral window. Since the Markarian survey is not line-selected, it is perhaps no surprise that not all of the objects from this survey were found by KISS. Of the 55 Case galaxies in

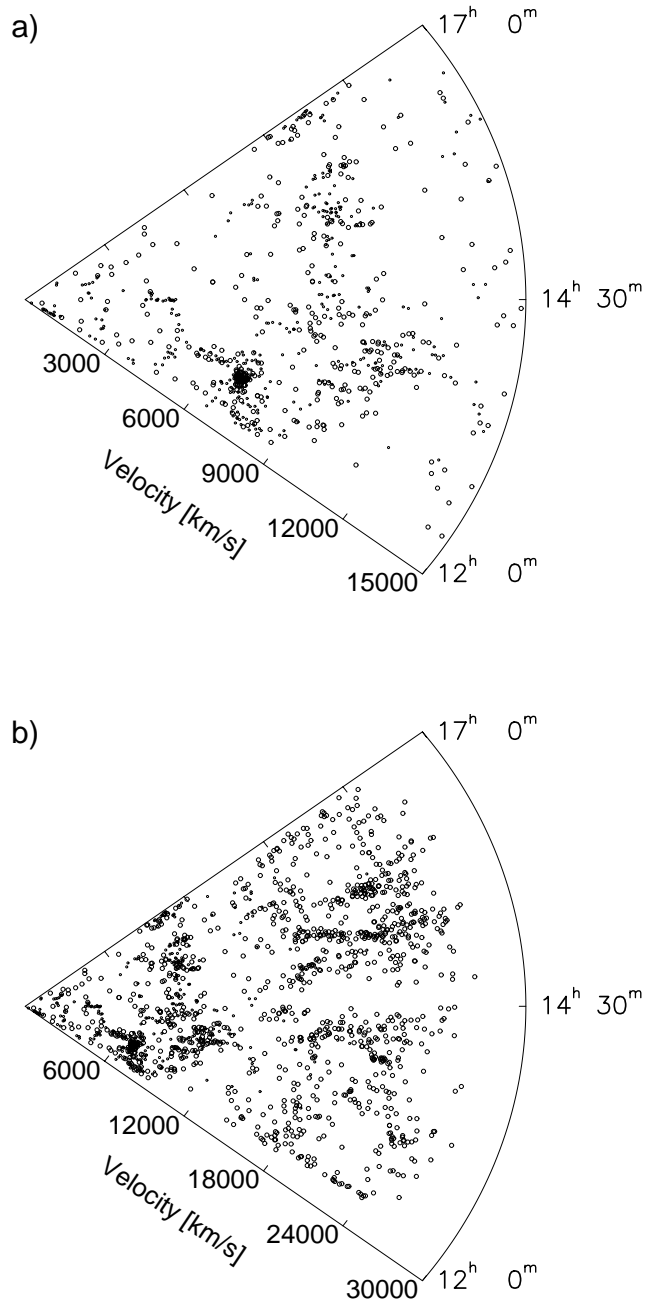


FIG. 9.— The spatial distribution of the KISS ELGs. The CGCG comparison sample is displayed as small dots, while the ELGs are larger, open symbols. (a) Velocities plotted out to  $15,000 \text{ km s}^{-1}$ . The ELGs are seen to trace the large-scale structures defined by the CGCG galaxies at low redshift. However, they exhibit the appearance of being less tightly clustered. A large number of ELGs are seen to fall in voids. (b) Velocities plotted out to  $30,000 \text{ km s}^{-1}$ . At larger distances the ELGs appear to reveal several structures not visible in the shallower CfA2 redshift catalog. The numbers of ELGs remains high out to  $\sim 27,000 \text{ km s}^{-1}$ , the point where the filter used for the survey truncates the sample. The lack of objects in the ELG distribution near  $14^{\text{h}} 40^{\text{m}}$  is caused by a  $15^{\text{m}}$  gap in the survey (see Section 2).

the KISS area, 39 were recovered by KISS (72%). We examined the 16 Case galaxies not recovered by KISS, and found that 11 are listed in the Case Survey papers as being color-selected, while the remaining five are all listed as having questionable (w? or w:) line detections. Spectroscopy of 61 Case galaxies by Salzer *et al.* (1995) in the red portion of the spectrum found that 31% had H $\alpha$  equivalent widths less than 30 Å. Hence, it would appear that the non-detected Case galaxies are simply the weak-lined subsample of the Case survey, to which KISS is not sensitive.

## 5. SUMMARY

We present the first list of emission-line galaxy candidates from the KPNO International Spectroscopic Survey. KISS is an objective-prism survey, similar in nature to a number of important surveys carried out in the past using Schmidt telescopes and photographic plates. The crucial improvement incorporated into KISS is the use of a CCD as the detector. This allows us to detect fainter ELGs than previous surveys. Our specially chosen filters also allow us to detect emission lines out to higher redshifts than did most previous line-selected surveys. The combination of higher sensitivity, lower noise, and larger volumes surveyed yield huge improvements in the depth of the resulting survey. KISS finds 181 times more AGN and starburst galaxy candidates per unit area than did the Markarian (1967) survey, and 32 times more than the UCM survey (Zamorano *et al.* 1994).

This first installment of KISS includes 1128 ELG candidates selected from 54 red survey fields covering a total of 62.2 deg<sup>2</sup>. The KISS catalog has a surface density of over 18 galaxies per deg<sup>2</sup>. The primary emission line we are sensitive to is H $\alpha$ . The survey follows a narrow strip across the sky at a declination of  $\delta(1950) = 29^\circ 30'$  and spanning the RA range 12<sup>h</sup> 15<sup>m</sup> to 17<sup>h</sup> 0<sup>m</sup>. This region was chosen to overlap the Century Redshift survey (Geller *et al.* 1997). For each object in the catalog we tabulate accurate equatorial coordinates, B & V photometry, and estimates of the redshift and line strength measured from the objective-prism spectra. Also provided are finder charts and extracted spectral plots for all galaxies. In addition to the main survey list, we include a supplementary list of 189 ELG candidates with weaker (lower significance) emission lines.

Since the survey data themselves provide such a large amount of observational data for each KISS ELG, we are able to develop a fairly complete picture of the survey constituents even before follow-up spectral information is available. The median apparent magnitude of the sample is  $B = 18.08$ , which is substantially fainter than previous ELG surveys. Objects fainter than  $B = 20$  are routinely cataloged.

Measurement of the line strengths in the objective-prism spectra show that KISS is sensitive to objects with H $\alpha$  + [N II] equivalent widths of less than 20 Å, and that most objects with  $EW > 30$  Å are detected. The median line flux of the KISS sample is more than three times lower than that of the UCM survey (Gallego *et al.* 1996). The luminosity distribution of the KISS ELGs is dominated by intermediate- and low-luminosity galaxies, although luminous AGN and starbursting galaxies are also represented. The median absolute magnitude of  $M_B = -18.96$  is characteristic of a small spiral galaxy or large Magellanic irregular, and underscores the fact that strong-lined galaxies of the type cataloged by KISS tend to be less luminous than the types of objects found in more traditional magnitude-limited samples.

Despite the fact that one can learn a great deal about each KISS object from the survey data alone, detailed follow-up spectra are still required to get a more complete picture. For example, one cannot distinguish between AGN and star-formation activity in the KISS galaxies based on the objective-prism spectra. Further, the redshifts derived from the KISS spectral data are too coarse to be used in detailed spatial distribution studies (e.g., Lee, Salzer & Gronwall 2001). We are in the process of obtaining spectra for a large number of KISS ELGs in order to better assess the nature of the individual galaxies, as well as to allow for a wide range of science applications, many of which are outlined in Paper I.

We gratefully acknowledge financial support for the KISS project through NSF Presidential Faculty Award to JJS (NSF-AST-9553020), which was instrumental in allowing for the international collaboration. Additional support for this project came from NSF grant AST-9616863 to TXT, and from Kitt Peak National Observatory, which purchased the special filters used by KISS. Summer research students Michael Santos, Laura Brenneman, and Erin Condy, supported by the Keck Northeast Astronomy Consortium student exchange program, helped to reduce the survey data presented in the current paper. We are grateful to Vicki Sarajedini and Laura Chomiuk, who assisted in so many ways during the final production of this paper, and to Katherine Rhode for her critical reading of the manuscript. Several useful suggestions by the anonymous referee helped to improve the presentation of this paper. We thank the numerous colleagues with whom we have discussed the KISS project over the past several years, including Jesús Gallego, Rafael Guzmán, Rob Kennicutt, David Koo, and Daniel Kunth. Finally, we wish to thank the support staff of Kitt Peak National Observatory for maintaining the telescope and instrument

during the early years of the project, and the Astronomy Department of Case Western Reserve University

for taking over this role after 1997.

## APPENDIX

### SUPPLEMENTARY TABLE OF $4\sigma$ OBJECTS

As explained in Section 3, the main selection criterion used to decide whether or not an object is included in the KISS catalog is the presence of a  $5\sigma$  emission feature in its spectrum. Because of the high sensitivity of the survey data, many objects were detected with emission lines which were slightly weaker than this level. We made the decision to exclude such objects from the main survey lists, in order to preserve the statistically complete nature of the sample. It was felt that the high degree of reliability of the sample would be compromised somewhat if these objects were included. However, rather than ignore these weaker-lined ELG candidates entirely, we are publishing them in a supplementary table.

Listed in Table 2 are 189 ELG candidates that have emission lines detected at between the  $4\sigma$  and  $5\sigma$  level. The format of Table 2 is the same as for Table 1, except that the objects are now labeled with KISSRx numbers ('x' for extra). The full version of the table, as well as finder charts for all 189 KISSRx galaxies, are available in the electronic version of the paper.

The characteristics of the supplementary ELG sample are similar to those of the main survey ELGs, although with some predictable differences. The median  $H\alpha$  equivalent width is 19.3 Å, a factor of two below the value for the main sample. The KISSRx galaxies are somewhat fainter (median B magnitude of 18.6) and significantly redder (median  $B-V = 0.80$ ). Their median redshift is slightly higher than that of the main sample (0.070), and their median luminosity is slightly lower ( $-18.6$ ). Hence, the supplementary ELG list appears to be dominated by intermediate luminosity galaxies with a significantly lower rate of star-formation activity (lower equivalent widths, redder colors) than the ELGs in the main sample.

## REFERENCES

- Burstein, D., & Heiles, C. 1984, *ApJS*, 54, 33  
 Falco, E. E., Kurtz, M. J., Geller, M. J., Huchra, J. P., Peters, J., Berlind, P., Mink, D. J., Tokarz, S. P., & Elwell, B. 1999, *PASP*, 111, 438  
 Fukugita, M., Shimasaku, K., & Ichikawa, T. 1995, *PASP*, 107, 945  
 Gallego, J., Zamorano, J., Rego, M., Alonso, O., & Vitores, A. G. 1996, *A&AS*, 120, 323  
 Geller, M. J., Kurtz, M. J., Wegner, G., Thorstensen, J. R., Fabricant, D. G., Marzke, R. O., Huchra, J. P., Schild, R. E., & Falco, E. E. 1997, *AJ*, 114, 2205  
 Gronwall, C., Salzer, J. J., Brenneman, L., Condy, E., & Santos, M. 2000, in preparation  
 Gronwall, C., Salzer, J. J., McKinstry, K., & Wegner, G. 2001, in preparation  
 Herrero, J. L., Frattare, L. M., Salzer, J. J., Gronwall, C., & Kearns, K. 2000, *PASP*, submitted  
 Lee, J. C., Salzer, J. J., & Gronwall, C. 2001, *ApJ*, in preparation  
 Lee, J. C., Salzer, J. J., Law, D. A., & Rosenberg, J. L. 2000, *ApJ*, 536, 606  
 MacAlpine, G. M., Smith, S. B., & Lewis, D. W. 1977, *ApJS*, 34, 95  
 Markarian, B. E. 1967, *Astrofizika*, 3, 55  
 Markarian, B. E., Lipovetskii, V. A., & Stepanian, D. A. 1983, *Astrofizika*, 19, 29  
 Mazzarella, J. M., & Balzano, V. A. 1986, *ApJS*, 62, 751  
 Nilson, P. 1973, *Uppsala General Catalogue of Galaxies*, (Uppsala: Roy. Soc. Sci. Uppsala)  
 Pérez-González, P. G., Zamorano, J., Gallego, J., & Gil de Pez, A. 2000, *A&AS*, 141, 409  
 Pesch, P., & Sanduleak, N. 1983, *ApJS*, 51, 171  
 Popescu, C. C., Hopp, U., & Elsässer, H. 1997, *A&A*, 328, 756  
 Popescu, C. C., Hopp, U., Hagen, H. J., & Elsässer, H. 1996, *A&AS*, 116, 43  
 Pustil'nik, S., Ugryumov, A. V., Lipovetsky, V. A., Thuan, T. X., & Guseva, N. 1995, *ApJ*, 443, 499  
 Roberts, M. S., & Haynes, M. P. 1994, *ARA&A*, 32, 115  
 Rosenberg, J. L., Salzer, J. J., & Moody, J. W. 1994, *AJ*, 108, 1557  
 Salzer, J. J. 1989, *ApJ*, 347, 152  
 Salzer, J. J., Gronwall, C., Lipovetsky, V. A., Kniazev, A., Moody, J. W., Boroson, T. A., Thuan, T. X., Izotov, Y. I., Herrero, J. L., & Frattare, L. M. 2000, *AJ*, 120, 80 (Paper I)  
 Salzer, J. J., Gronwall, C., Lipovetsky, V. A., Kniazev, A., Sarajedini, V. L., Moody, J. W., Boroson, T. A., Thuan, T. X., Izotov, Y. I., Herrero, J. L., & Frattare, L. M. 2001, in preparation (KB1)  
 Salzer, J. J., MacAlpine, G. M., & Boroson, T. A. 1989, *ApJS*, 70, 479  
 Salzer, J. J., Moody, J. W., Rosenberg, J. L., Gregory, S. A., & Newberry, M. V. 1995, *AJ*, 109, 2376  
 Schechter, P. L. 1976, *ApJ*, 203, 297  
 Smith, M. G., Aguirre, C., & Zelman, M. 1976, *ApJS*, 32, 217  
 Surace, C., & Comte, G. 1998, *A&AS*, 133, 171  
 Wasilewski, A. J. 1983, *ApJ*, 272, 68  
 Zamorano, J., Rego, M., Gallego, J., Vitores, A. G., González-Riestra, R., & Rodríguez-Caderot, G. 1994, *ApJS*, 95, 387  
 Zwicky, F., Herzog, E., Kowal, C. T., Wild, P., & Karpowicz, M. 1961–1968, *Catalogue of Galaxies and Clusters of Galaxies*, (Pasadena: CIT) (CGCG)



TABLE 1  
LIST OF CANDIDATE ELGS

KISSR # (1)	Field (2)	ID (3)	R.A. (J2000) (4)	Dec. (J2000) (5)	B (6)	B-V (7)	$z_{KISS}$ (8)	Flux <sup>a</sup> (9)	EW [Å] (10)	Qual. (11)	Comments (12)
1	F1215	4723	12 15 06.9	29 01 10.0	17.35	0.53	0.0266	120	53	1	
2	F1215	4362	12 15 23.9	29 10 46.8	16.79	0.68	0.0300	202	27	1	
3	F1215	4188	12 15 36.9	28 59 29.4	16.41	0.81	0.0283	204	23	1	
4	F1215	3026	12 16 46.4	29 26 10.5	18.04	0.78	0.0619	141	44	1	
5	F1215	2774	12 17 10.1	28 57 53.1	19.02	0.52	0.0590	53	46	2	
6	F1215	2005	12 17 56.9	29 07 16.6	16.88	0.63	0.0510	180	23	1	
7	F1215	1851	12 18 11.9	28 43 39.0	18.55	0.72	0.0837	52	40	1	
8	F1215	1748	12 18 12.2	29 15 06.3	16.60	0.60	0.0269	149	28	1	CG 167, Was 51
9	F1215	1639	12 18 19.3	29 15 13.3	15.97	0.88	0.0492	309	23	1	UGC 7342
10	F1215	1628	12 18 20.2	29 14 48.2	17.80	0.82	0.0696	339	71	1	
11	F1215	1631	12 18 23.4	28 58 10.7	17.14	0.65	0.0779	464	90	1	
12	F1215	1627	12 18 23.5	28 58 29.4	17.16	0.45	0.0767	459	110	1	
13	F1215	1485	12 18 33.1	28 56 33.1	18.56	0.62	0.0763	89	73	1	
14	F1215	1187	12 18 41.8	29 41 27.1	18.39	0.79	0.0784	85	54	1	
15	F1215	1040	12 18 58.6	29 09 03.4	20.52	0.84	0.0582	26	58	3	
16	F1215	886	12 19 06.3	29 22 04.8	18.62	0.88	0.0703	54	23	2	
17	F1215	978	12 19 06.8	28 45 39.8	18.15	0.93	0.0760	128	50	1	
18	F1215	767	12 19 18.0	29 05 59.9	18.50	0.67	0.0839	75	49	1	
19	F1215	745	12 19 18.7	29 10 34.0	21.36	0.72	0.0577	31	39	3	
20	F1215	788	12 19 21.4	28 42 04.9	19.66	0.67	0.0739	42	82	2	
21	F1215	430	12 19 34.1	29 47 53.1	18.36	0.64	0.0671	133	59	1	
22	F1215	509	12 19 37.6	28 55 55.1	19.68	0.85	0.0796	32	46	3	
23	F1215	504	12 19 39.1	28 51 40.9	19.05	1.14	0.0831	73	45	2	
24	F1215	387	12 19 44.2	29 13 06.7	18.39	0.80	0.0843	91	42	1	
25	F1215	361	12 19 49.2	28 58 24.8	18.59	1.09	0.0825	78	33	2	
26	F1215	226	12 19 49.9	29 40 17.4	19.99	1.43	0.0157	96	80	3	
27	F1215	228	12 19 50.6	29 36 52.3	11.46	0.99	0.0092	1254	9	3	UGC 7377
28	F1220	3903	12 20 01.4	29 28 07.6	18.43	0.65	0.0761	103	66	1	
29	F1220	3863	12 20 06.8	29 16 50.3	11.53	0.99	0.0065	1715	3	2	UGC 7386, CG 170
30	F1220	3801	12 20 16.2	28 51 19.4	19.08	0.98	0.0799	40	52	2	

Note.— The complete version of this table is presented in the electronic edition of the Journal. A portion is shown here for guidance regarding its content and format.

<sup>a</sup>Units of  $10^{-16}$  erg/s/cm<sup>2</sup>

TABLE 2  
LIST OF  $4\sigma$  CANDIDATE ELGs

KISSRx # (1)	Field (2)	ID (3)	R.A. (J2000) (4)	Dec. (J2000) (5)	B (6)	B-V (7)	$z_{KISS}$ (8)	Flux <sup>a</sup> (9)	EW [Å] (10)	Qual. (11)	Comments (12)
1	F1215	4333	12 15 26.2	29 06 48.6	17.74	0.54	0.0301	65	36	1	
2	F1220	2840	12 21 23.6	28 40 15.8	18.64	1.01	0.0738	39	25	2	
3	F1220	945	12 23 49.3	29 43 04.1	18.68	0.57	0.0645	32	30	2	
4	F1225	5035	12 25 19.0	28 50 12.2	22.91	2.48	0.0017	60	129	2	
5	F1225	48	12 30 03.0	29 04 17.3	18.72	0.69	0.0639	47	37	2	
6	F1235	1105	12 37 56.7	29 41 06.2	19.74	0.33	0.0545	19	44	3	
7	F1240	4669	12 40 01.8	29 32 09.8	21.08	1.83	0.0833	37	60	2	
8	F1245	1131	12 48 51.2	28 58 04.9	17.33	0.98	0.0346	30	7	1	
9	F1250	2820	12 51 24.9	29 23 52.2	18.39	1.00	0.0294	46	24	2	
10	F1250	2180	12 52 14.8	29 25 43.3	16.33	0.70	0.0608	69	8	2	
11	F1255	1837	12 57 49.9	29 39 15.4	15.25	0.42	0.0133	57	5	1	UGC 8076
12	F1300	2861	13 01 09.6	29 03 55.9	18.59	0.19	0.0300	27	34	2	
13	F1300	2494	13 01 34.1	28 58 55.9	18.58	0.92	0.0849	48	21	2	
14	F1300	675	13 03 47.4	29 42 39.7	17.93	0.51	0.0866	61	37	2	
15	F1300	388	13 04 22.1	28 45 52.9	18.58	0.19	0.0190	34	43	2	
16	F1305	5898	13 05 31.4	29 38 44.7	19.95	1.91	0.0605	54	49	2	
17	F1310	151	13 14 52.8	28 43 21.9	17.42	0.37	0.0763	26	14	2	
18	F1315	4390	13 15 06.4	29 36 58.7	17.27	1.16	0.0623	212	29	2	
19	F1315	3896	13 15 50.6	28 37 16.8	19.24	0.84	0.0203	36	27	3	
20	F1325	4575	13 24 54.2	28 49 49.8	17.67	0.25	0.0559	62	37	2	
21	F1330	3167	13 32 24.8	29 05 04.7	17.77	0.75	0.0447	43	12	2	
22	F1330	466	13 34 38.3	29 27 38.5	18.63	0.70	0.0393	21	17	2	
23	F1335	3771	13 35 37.1	28 58 17.3	18.98	0.59	0.0369	38	38	2	
24	F1335	1550	13 38 14.1	29 43 07.2	18.69	0.65	0.0367	25	15	2	
25	F1340	3564	13 41 03.4	29 19 42.7	18.55	1.24	0.0827	16	6	3	
26	F1345	4781	13 44 50.1	29 13 55.5	17.69	0.94	0.0298	35	8	2	
27	F1345	2614	13 46 56.4	29 39 29.3	17.46	0.63	0.0294	87	26	2	Mk 274
28	F1345	2220	13 47 25.2	29 37 31.9	18.36	0.64	0.0775	97	57	1	
29	F1345	1931	13 47 54.7	28 41 06.5	17.63	1.12	0.0277	67	10	1	
30	F1345	875	13 49 04.0	28 48 59.3	17.97	0.34	0.0695	29	14	2	

Note.— The complete version of this table is presented in the electronic edition of the Journal. A portion is shown here for guidance regarding its content and format.

<sup>a</sup>Units of  $10^{-16}$  erg/s/cm<sup>2</sup>